Astron. Astrophys. 322, 66–72 (1997)

ASTRONOMY AND ASTROPHYSICS

ROSAT/HRI study of the optically rich, lensing cluster Cl 0500-24

Sabine Schindler[1,2] **and Joachim Wambsganss**[3]

[1] MPI für extraterrestrische Physik, Giessenbachstr., D-85748 Garching, Germany (sas@mpa-garching.mpg.de)
[2] MPI für Astrophysik, Karl-Schwarzschild-Str. 1, D-85748 Garching, Germany
[3] Astrophysikalisches Institut Potsdam, An der Sternwarte 16, D-14482 Potsdam, Germany (jwambsganss@aip.de)

Received 15 July 1996 / Accepted 16 November 1996

Abstract. An analysis of a ROSAT/HRI observation of the optically rich, gravitationally lensing galaxy cluster Cl 0500-24 (or Abell S0506) is presented. The X-ray luminosity and the morphology of the extended X-ray emission support the view that Cl 0500-24 consists of two subclusters at a velocity difference of $\Delta v \approx 3200$ km/s that happen to lie along the line of sight and are probably physically unrelated. The X-ray emission is mainly correlated with one of the subclusters – the northern subconcentration at redshift $z = 0.327$. We show that the X-ray luminosity of this supposedly rich cluster is relatively low at $3.1^{+0.6}_{-0.4} \times 10^{44}$ erg/s in the ROSAT band ($5.6^{+4.2}_{-2.0} \times 10^{44}$ erg/s bolometric) indicating that there is no tight correlation between X-ray luminosity and optical richness. The derived total mass of the cluster of $(1.5 \pm 0.8) \times 10^{14} M_\odot$ (within 1 Mpc of the X-ray maximum) is very low even when assigning it only to one subcluster. The gas mass within the same radius is $0.5 \times 10^{14} M_\odot$, corresponding to a high gas mass fraction of $30^{+30}_{-10}\%$.

Key words: galaxies: clusters: individual: Cl 0500-24 – galaxies: clusters: individual: A S0506 – intergalactic medium – dark matter – X-rays: galaxies

1. Introduction

The cluster Cl 0500-24 is an optically rich, very compact cluster of galaxies (Giraud 1988) at a medium redshift of $z \approx 0.32$ (in Abell et al. (1989) it is listed as supplementary cluster S0506). There are 95-100 galaxies brighter than V = 23 within a radius of $\approx 0.55 h_{50}^{-1}$Mpc. The average density, $N_{0.5}$, defined as the number of bright galaxies,$m \leq m_3 + 2$ (where m_3 is the magnitude of the third brightest galaxy) projected within a radius of $0.5 h_{50}^{-1}$Mpc is 31-36. This means that Cl 0500-24 appears richer than the well studied giant gravitational arc cluster Abell 370, for which $N_{0.5} = 28$ (see Mellier et al. 1988). Cl 0500-24 contains a large fraction of blue galaxies, and has a quite high line of sight velocity dispersion of $\sigma = 1375$km/s, based on redshifts of 22 cluster galaxies (Giraud 1990). The cluster "apparently has a triple core" (Giraud 1988) so it is to be expected that an X-ray map will identify substructure. Infante et al. (1994) found a bimodal distribution in the galaxy velocities, enhancing this view that the cluster consists of subclumps.

The known redshifts of the galaxies in Cl 0500-24 cover quite a broad range. Infante et al. (1994) showed that the velocity distribution (26 measured galaxies) is bimodal with two peaks at $v_1 = 94817$ km/s and $v_2 = 97987$ km/s. The velocity difference ($\Delta v = v_2 - v_1 = 3170$ km/s) is much larger than the one-dimensional velocity dispersions of the two sub-clumps ($\sigma_1 = 917 \pm 208$ km/s, $\sigma_2 = 1152 \pm 214$ km/s). This double nature of the cluster was supported by Infante et al. (1994)'s group finding algorithms. So it appears that Cl 0500-24 is not one rich cluster, but rather two subclusters along the line of sight.

The most striking feature in Cl 0500-24 is a straight, blue arc with a length of about 14 arcseconds, which is about 22 arcseconds away from the apparent cluster centre. A gravitational lens model for this arc (Wambsganss et al. 1989) finds very naturally a strongly elongated image of a background galaxy at the position of the arc with the correct orientation. This model predicts a mass of about $1.4 \times 10^{14} M_\odot$ for the (projected) inner part of the cluster, i.e. for a circle around the apparent centre C with radius centre-arc (cf. Giraud 1990). Equivalently, a cluster modeled as a singular isothermal sphere with a velocity dispersion of 1200 km/s is necessary to produce an arc with this length at this location. The redshift of the arc was measured to be $z_{arc} = 0.913$ (Giraud 1996) confirming the gravitational lens scenario quite satisfactorily. So far no arclets or weak lensing signature have been reported in this cluster.

Here we present X-ray observations of Cl 0500-24 with the ROSAT/HRI (Trümper 1983). We show the morphology as it appears in X-rays, we determine an X-ray profile and the X-ray luminosity, and we estimate the mass of the X-ray emitting gas and the total mass of the cluster. Finally, we discuss our results and compare them with other X-ray/lensing clusters. Throughout this paper we use $H_0 = 50$km/s/Mpc, Ω_0=1 and q_0=0.5.

Send offprint requests to: Sabine Schindler

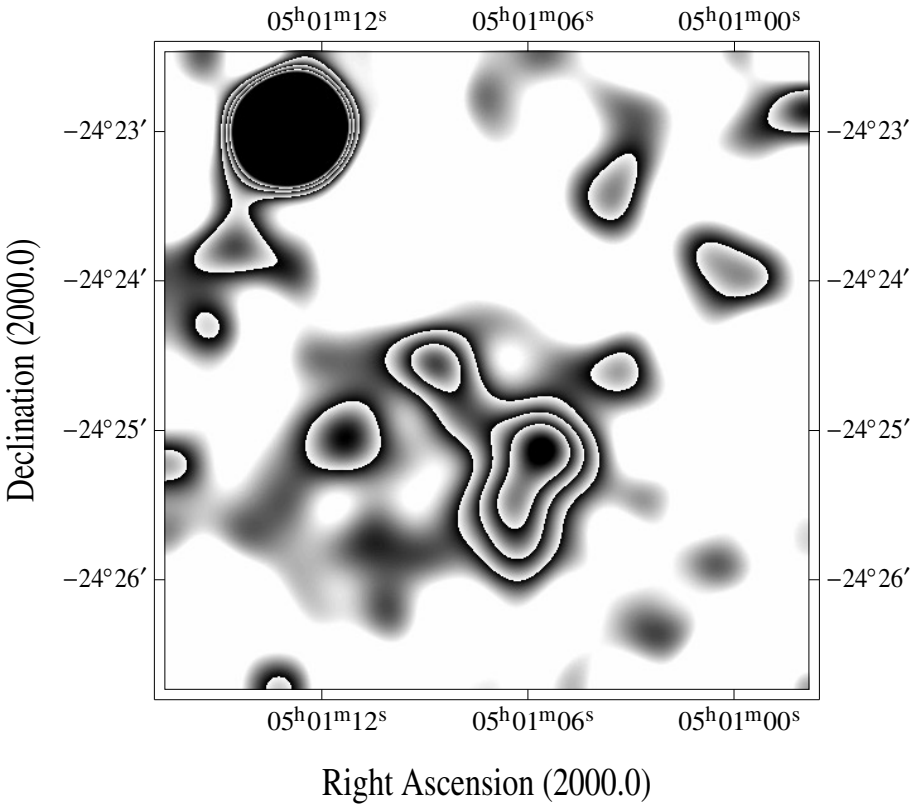

Fig. 1. ROSAT/HRI image of the cluster Cl 0500-24. It is smoothed with a Gaussian filter of σ = 10 arcseconds. The cluster has a clumpy structure with an extension south of the maximum and additional emission in the north-east and in the east. The bright X-ray source in the upper left corner is not associated with the cluster.

2. X-ray data

Cl 0500-24 was observed with the ROSAT/HRI in a pointed observation with an exposure time of 37756 s between February 8^{th} and 13^{th}, 1995.

The positioning of the observation can be checked with a point-like source which coincides with a star of blue magnitude 16.8 at a position $\alpha = 05^h01^m26.0^s$, $\delta = -24°17'31''$ (J2000). From this correspondence we infer that the positional accuracy of the pointing is very good (estimated error $\leq$ 4 arcseconds). The total number of source photons for the cluster Cl 0500-24 is 440.

As the cluster emission is not very strong we follow a two-fold strategy. In addition to the straightforward analysis of the full data set, we try to improve the signal-to-noise ratio by skipping the intervals with enhanced background. In practice, we bin the data to intervals of 100 s. Subsequently, we drop the high background intervals with more than 500 counts / 100 s. The remaining time intervals with the "cleaned data" cover 57% of the original exposure time. The cleaned data set contains 270 source photons.

2.1. Morphology

Because of the limited number of photons from the cluster the observed morphology is influenced by statistical fluctuations. In Fig. 1 we present an image smoothed with a Gaussian filter of σ = 10 arcseconds for a qualitative impression of the morphology. The main maximum of an image smoothed with a Gaussian of σ = 5 arcseconds is at $\alpha = 05^h01^m05.6^s$, $\delta = -24°25'03''$ (J2000). It corresponds to a position between the galaxies N and S (nomenclature according to Giraud (1990)) which are identified by Infante et al. (1994) as the centre of one of two subconcentrations. In an image smoothed with a Gaussian of σ = 10 arcseconds the X-ray maximum is also very close to these galaxies (see Fig. 2). The X-ray emission is elongated southward towards galaxy A. A second maximum of the X-ray emission can be seen in the north-east at $\alpha = 05^h01^m09^s$, $\delta = -24°24'31''$ (J2000), close to galaxy # 12 (cf. Infante et al. 1994). There is no extra emission associated with the second optical centre C. All these features are "robust" in that they show up both in the "cleaned" and in the "non-cleaned" data.

The galaxies are assigned to two subclusters centred on galaxy N and on galaxy C, respectively, by Infante et al. (1994) according to their velocities from Giraud (1990) and Infante et al. (1994). The distribution of "N galaxies" is much better correlated with the X-ray emission than the distribution of "C galaxies" (see Fig. 2). This is a first hint that we see only (or mainly) the N subcluster in X-rays.

In Fig. 3 the X-ray morphology is compared with the galaxy density (Infante, private communication) for all galaxies (while in Fig. 2 only galaxies with measured velocities were included). The contour lines of the luminosity weighted galaxy density show again the two main concentrations around N and C, out of which only N is correlated with X-rays. Another maximum in the galaxy density in the north-east is situated between two X-ray blobs and is probably belonging to the N concentration

because there are three "N galaxies" in this region, i.e. again no indication for any emission from the C subcluster.

About 2.6 arcminutes north-east of the cluster centre is a point-like source (see Fig. 1) at $\alpha = 05^h01^m13^s$, $\delta = -24°22'59''$ (J2000). It has a countrate of 8.6×10^{-3} counts/s. The position of this source corresponds within 10 arcseconds to the radio source PMN0501-2422 which is listed in Griffith et al. (1994) with a 4850 MHz flux density of 154 mJy. Looking for an optical counterpart in the Southern Digitized Sky Survey we find a faint object at about 4 arcseconds distance; it cannot be distinguished whether it is a stellar object or a galaxy.

2.2. Luminosity

The X-ray emission can be traced out to a radius of 2.5 arcminutes (860 kpc at distance of cluster). As summarized in Table 1, we find a countrate of 0.012 ± 0.001 counts/s within this radius. To convert this countrate to a luminosity we assume a typical metallicity of 0.35 solar (Arnaud et al. 1992; Ohashi 1995) and a Galactic hydrogen column density of 7.12×10^{22} cm^{-2} (Dickey & Lockman 1990). As there is no possibility to derive a gas temperature with the HRI we assume a typical cluster temperature of 4 keV which is also consistent with the $L_X - T$ relation (Edge & Stewart 1991a; David et al. 1993; White 1996). With these values the luminosity in the ROSAT band (0.1 - 2.4 keV) is $3.1^{+0.6}_{-0.4} \times 10^{44}$ erg/s and the bolometric luminosity is $5.6^{+4.2}_{-2.0} \times 10^{44}$ erg/s. The errors include the uncertainties of the countrate and an assumed temperature range between 1 and 10 keV.

2.3. Profile

Because of the limited number of photons and the non-spherical appearance of the X-ray contours, the radial profile of the X-ray emission is not very well determined (Fig. 4). Nevertheless, we try to fit a β-model to the surface brightness (following Cavaliere & Fusco-Femiano 1976; Jones & Forman 1984)

$$\Sigma(r) = \Sigma_0 \left(1 + \left(\frac{r}{r_c}\right)^2\right)^{-3\beta+1/2}, \qquad (1)$$

where Σ_0 is the central surface brightness, r_c is the core radius, and β is the slope parameter. The best fit values averaged over a number of fits with or without "cleaning" and with different binning centred on $\alpha = 05^h01^m05.6^s$ $\delta = -24°25'03''$ (J2000) are $\Sigma_0 = 8 \times 10^{-3}$ counts/s/arcmin^2, $r_c = 0.09$ arcminutes (30 kpc) and $\beta = 0.4$, a very small β and a very small core radius. But the 1σ errors allow for a huge range of about 0.3 to 1.0 for β and 0 to 1.5 arcminutes (0 to 500 kpc) for the core radius.

2.4. Mass determination

The parameters of the β-model can be used to make a deprojection of the 2D image to derive the three dimensional density distribution. The profile of the integrated gas mass is shown in Fig. 5. Within a radius of 1 Mpc the gas mass amounts to $0.46 \times 10^{14} M_\odot$. As the emissivity of the gas in the ROSAT energy band is almost independent of the temperature (within the temperature range of 2-10 keV it changes only by 6%), the derived gas density distribution is affected very little by the uncertainty of the temperature estimate. The only uncertainty are local unresolved inhomogeneities or substructure which result in an overestimation of the gas mass. Therefore, the value given above is strictly speaking an upper limit.

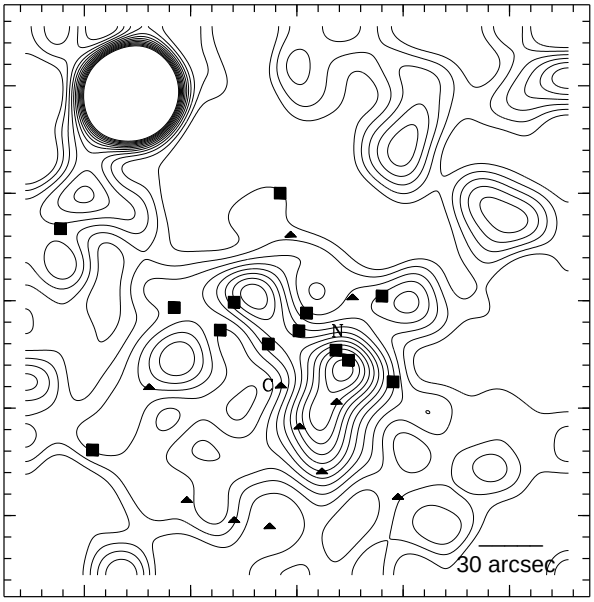

Fig. 2. Cluster galaxies assigned to the subclusters N and C by Infante et al. (1994) superimposed on the X-ray contours (smoothed with a Gaussian filter of σ = 10 arcseconds). Triangles: galaxies assigned to subcluster C, squares: galaxies assigned to subcluster N. The size of the image is the same as in Fig. 1. One tickmark corresponds to 10 arcseconds or 57 kpc. The contour levels have a linear spacing of 3.8×10^{-4}counts/s/arcmin^2. The highest contour corresponds to 9.2×10^{-3}counts/s/arcmin^2, the lowest to 5.0×10^{-3}counts/s/arcmin^2. The central galaxies of the subclusters are marked with N and C, respectively. The X-ray emission is well correlated with the subcluster centred on N, while there is hardly any correlation with the C subcluster. In particular, there is no extra emission at the position of the central galaxy C.

With the additional assumption of hydrostatic equilibrium, the integrated total mass can be calculated from the equation

$$M(r) = \frac{-kr}{\mu m_p G} T \left(\frac{d\ln\rho}{d\ln r} + \frac{d\ln T}{d\ln r}\right), \qquad (2)$$

where ρ and T are the density and the temperature of the intracluster gas, and r, k, μ, m_p, and G are the radius, the Boltzmann constant, the molecular weight, the proton mass, and the gravitational constant, respectively. For the temperature we use again the cluster temperature of 4 keV from the $L_X - T$ relation (Edge & Stewart 1991a; David et al. 1993; White 1996). When using the parameters of the various β-model fits with varying binning and with/out "cleaning" we find different mass profiles only in the central part (see Fig. 5). Beyond a radius of about 100 kpc

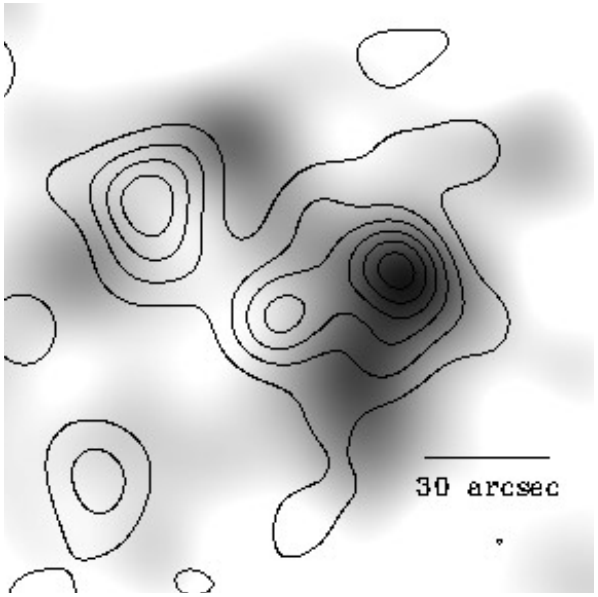

Fig. 3. Luminosity weighted galaxy densities (contours) from V magnitudes (Infante, private communication) smoothed with a Gaussian of σ = 8 arcseconds are superimposed on the X-ray emission (greyscales, same as the contours of Fig. 2). The size of the image is 2.5x2.5 arcminutes or 860x860 kpc.

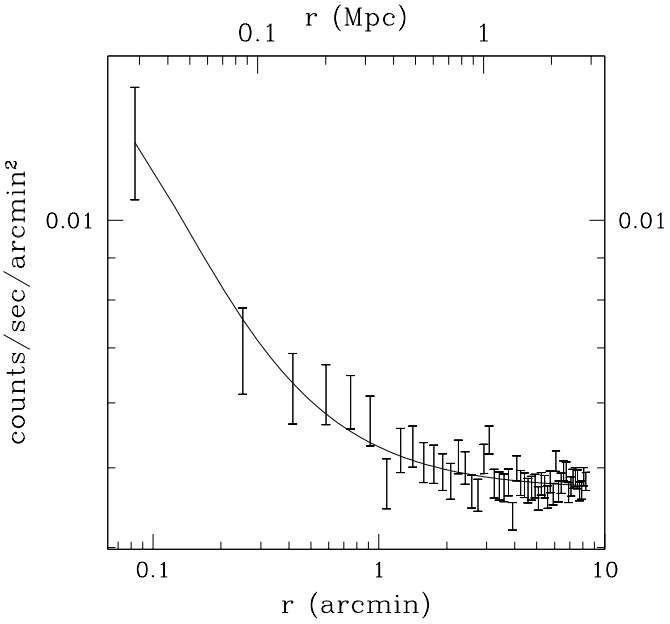

Fig. 4. Radial profile of the X-ray emission fitted with a β-model.

the various mass profiles are in good agreement. The error originating from the uncertainty in the temperature is certainly much larger. As the mass is proportional to the assumed temperature (see Eq. 2) we estimate that the error can amount to $\pm$50%.

The results are shown in Fig. 5. At a radius of 1 Mpc we find an integrated total mass of $(1.5 \pm 0.8) \times 10^{14} M_{\odot}$. The errors comprise a temperature range from 2 to 6 keV. This total mass yields a relatively high gas mass fraction of 30^{+30}_{-10}%. The gas mass fraction is decreasing when going to smaller radii. But as the gas mass fraction depends on β and β is not very well defined (see Sect. 2.3) this decrease may not be very significant. For completeness we also check the extreme (and unrealistic) parameters allowed from the surface profile fit r_c = 500kpc and β =1.0. The resulting integrated mass profile is steeper than the ones shown in Fig.5 crossing the other profiles at about 350 kpc. At 1 Mpc the total mass for these extreme parameters amounts to $3.6 \times 10^{14} M_{\odot}$.

The total mass (from the realistic parameters) is even smaller than the luminosity-weighted virial mass of $2.2 \times 10^{14} M_{\odot}$ of only the N concentration derived by Infante et al. (1994). (The X-ray mass converted to their H_0 = 60km/s/Mpc would be $1.3 \times 10^{14} M_{\odot}$.) This is another hint that the X-ray emitting gas traces the potential of only one subcluster.

For a comparison with mass estimates determined from the gravitational lensing effect, we also calculate the total mass of the cluster, as seen inside a certain angle, basically integrating a spherically symmetric three dimensional mass distribution in cylindrical shells with cylinder axis parallel to the line of sight or integrating the cluster surface mass density $\Sigma(\theta)$ outward (see Fig. 5). The total mass inside a circle with radius cluster centre-arc is $0.3 \times 10^{14} M_{\odot}$.

From the point lens model, Wambsganss et al. (1989) found a much larger value: $1.4 \times 10^{14} M_{\odot}$ (or a velocity dispersion of σ = 1200 km/s for an isothermal sphere model); here the now measured arc redshift of z_{arc} = 0.913 (Giraud 1996) and a distance between centre of lens and arc of 22 arcsec was used. Obviously, the mass from the lens model is considerably higher than the mass obtained here when integrating outward the total mass derived from the X-ray emission even when taking into account the large X-ray mass error of $\pm$50%. This discrepancy of a factor 4-5 does not necessarily come from a wrong assumption in one of the two mass determination methods. It can have various reasons. The two mass estimates are not directly comparable because they use different centres: the X-ray mass is centred on the X-ray maximum which is located close to galaxy N while the lensing model has an assumed centre close to 'C'. Furthermore, the two methods to determine the mass are sensitive to different things: the gravitational lens effect integrates all matter along the line of sight, while the X-ray mass determination is most sensitive to the (square of the) highest density regions in the centre of the cluster. Qualitatively the discrepancy of a large lensing mass and a small X-ray mass points in the same direction that Cl 0500-24 consists of two subclusters, of which the lensing "feels" the total mass, whereas the X-ray are indicative only of one subclump. But any more detailed comparison would require a much more detailed model of the cluster lens, which could possibly be obtained from a deep exposure of the cluster and subsequent analysis of arclets and the weak lensing effect.

Table 1. Summary of the X-ray properties of Cl 0500-24 in comparison to other optically rich clusters Cl 0939-4713 and Cl 0016+16. The numbers for Cl 0939-4713 are taken from Schindler & Wambsganss (1996), the numbers for Cl 0016+16 from Neumann & Böhringer (1996). The countrates for Cl 0939-4713 and Cl 0016+16 are converted from PSPC countrates.

	Cl 0500-24	Cl 0939-4713	Cl 0016+16
HRI countrate(0.1-2.4keV) [counts/s]	0.012 ± 0.001	0.028 ± 0.001	0.029 ± 0.001
L_X(0.1-2.4keV) [erg/s]	$3.1^{+0.6}_{-0.4} \times 10^{44}$	$7.9 \pm 0.3 \times 10^{44}$	$1.9 \pm 0.1 \times 10^{45}$
L_X(bol) [erg/s]	$5.6^{+4.2}_{-2.0} \times 10^{44}$	$1.1 \pm 0.05 \times 10^{45}$	$5.0^{+0.9}_{-0.6} \times 10^{45}$
$M_{gas}(r < 1\text{Mpc})$	$0.5 \times 10^{14} M_\odot$	$0.84 \times 10^{14} M_\odot$	$1.3 \times 10^{14} M_\odot$
$M_{tot}(r < 1\text{Mpc})$	$1.5 \pm 0.8 \times 10^{14} M_\odot$	$\gtrsim 2.6^{+1.2}_{-0.6} \times 10^{14} M_\odot$	$6.3 \pm 1.9 \times 10^{14} M_\odot$
gas mass fraction ($<$ 1Mpc)	$30^{+30}_{-10}\%$	25 - 50%	$20^{+10}_{-4}\%$
redshift	0.32	0.41	0.55

3. Discussion and conclusions

The X-ray luminosity of Cl 0500-24 is very moderate. Actually, it is quite small for a "rich" cluster of galaxies. The Abell Cluster A370 (at a comparable redshift), which optically appears about equally rich as Cl 0500-24, is roughly ten times more luminous in X-rays (Lea & Henry 1988; Fabricant et al. 1991; Bautz et al. 1994). Does this show that there is a wide spread of X-ray luminosities for clusters that appear similarly rich optically?

We argue that the X-ray emission of Cl 0500-24 originates mainly from the northern subclump. But even when comparing the bolometric luminosity of Cl 0500-24 only with the velocity dispersion of the northern subcluster, it is unexpectedly low (Edge & Stewart 1991b). This indicates at least a moderate spread in the optical richness versus X-ray luminosity relation.

There are other examples that illustrate this, e.g. the two distant clusters Cl 0939+4713 and Cl 0016+16, which are both optically very rich (Dressler 1994; Koo 1981) but have quite different bolometric X-ray luminosities (Schindler & Wambsganss 1996; Neumann & Böhringer 1996). Various properties of these two clusters, along with those of Cl 0500-24, are compiled in Table 1 for comparison.

The subcluster around galaxy C is even less X-ray luminous. Judging from optical data alone, it is well justified to assign the centre of the subcluster with redshifts peaking at v_1 (cf. introduction) to the position of galaxy C. Galaxy C is the most luminous galaxy of all galaxies with redshifts around v_1, and its velocity is very close to the maximum of their velocity distribution. To be more quantitative about the X-ray luminosity of subcluster C, we subtracted a spherically symmetric profile (see Fig. 4) centred on the X-ray maximum from the total X-ray emission. The remaining X-ray flux at the position of C has a count rate of $(0.0 \pm 0.1) \times 10^{-3}$ counts/s/arcmin^2, above a background of 4.6×10^{-3} counts/s/arcmin^2. If subcluster C has any X-ray emission at all, it is extremely small. Scaling from the difference in measured velocity dispersions, the mass difference of the subclusters is by far not sufficient to account for the different X-ray luminosities. Subcluster C must have a much lower gas mass fraction than subcluster N.

Given the bimodal velocity distribution of the galaxies in Cl 0500-24 (cf. Introduction), there are two possibilities for the spatial distance of the subclusters along the line of sight. One possible scenario is that the two subclusters have a physical distance which is smaller than that corresponding to the redshift difference, and are in the process of colliding. The other possibility is that the two subclusters are relatively unrelated and the different velocities are caused mainly by the Hubble flow. In this case they have a distance of more than 60 Mpc.

Unfortunately, the X-ray morphology does not give a final answer to the question whether the two subclusters are interacting or not, for two reasons: Firstly, the HRI image is affected by statistical fluctuations as it contains only 440 source counts. Secondly, a collision along a direction close to the line of sight cannot be easily distinguished from a virialized cluster by looking at the X-ray image only (Schindler & Müller 1993).

As the relative velocity of the subclusters of almost 3200 km/s is very high, in a merging scenario the subclusters would have to pass right through each other along the line of sight. In fact, the projected distributions of the galaxies with redshift z_2 preferentially north, and with z_1 preferentially south indicates, that such a collision could not be exactly along the line of sight, but with some angle relative to it. So the velocity difference is only the contribution projected onto the line of sight, and the real 3dim relative velocity would be even larger than the measured difference. N-body models show that relative velocities around 3000 km/s or more are reached only during a very short period of time as the subclusters pass through each other (Schindler & Böhringer 1993; Huss et al. 1996). If the

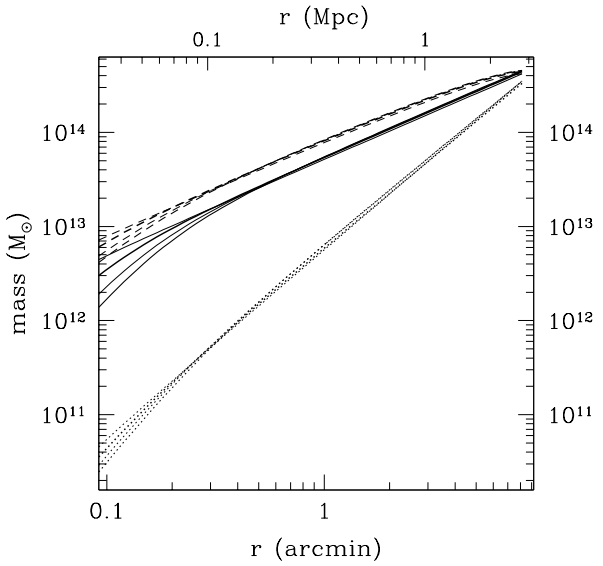

Fig. 5. Mass profile of Cl 0500-24. The dotted lines show the integrated gas mass, the solid lines the integrated total mass. Profiles for data with/out "cleaning" and with different binning are plotted. For the different profiles the following parameters are used r_c = 1.4arcsec, β = 0.34; r_c = 7.1arcsec, β = 0.37; r_c = 9.1arcsec, β = 0.37; r_c = 4.5arcsec, β = 0.36 (from thin to thick lines). In the inner region the scatter is quite large because of the limited number of photons. But beyond a radius of 100 kpc the profiles agree well. For comparison with mass determinations by the gravitational lens effect, the dashed lines depict the integrated surface mass density.

subclusters are just passing through each other, an X-ray emission enhanced by about a factor of two relative to a quiescent state is expected during a collision (Schindler & Müller 1993). However, given the low observed X-ray luminosity, and the fact that it is very unlikely that we see Cl 0500-24 exactly in this extreme short phase corresponding to such an encounter with high relative velocity we conclude that it is extremely unlikely that the two subclumps are currently undergoing such a collision. Due to these reasons we conclude that the scenario of two non-interacting subclusters at a large distance is much more likely.

This view of two unrelated subclusters that appear as one richer cluster due to the projection is also supported both by the morphology and the luminosity of the X-ray emission of the cluster. The X-rays originate from regions that are related to the subclump around N with galaxy velocities peaking at v_2. There is no significant detection from the supposed centre of the cluster near galaxy C (cf. Giraud 1990) or other galaxies at redshift z_1.

New insight into the dynamical state of Cl 0500-24 may come from a temperature measurement with ASCA. During a collision the intra-cluster gas is heated (Schindler & Müller 1993) so that in this case a higher temperature than the 4 keV from the $L_X - T$ relation is expected.

The mass assigned by Infante et al. (1994) to the more massive subclump around N at z_2 is even higher than the X-ray mass determined here. That can be another indication that the X-rays trace the potential of only one subcluster while the southern subcluster around galaxy C apparently does not affect the X-ray mass determination. The mass found by Wambsganss et al. (1989) for the cluster from a simple gravitational lens model for the straight arc is higher than the X-ray mass determined here. This also fits into this picture of two subclusters qualitatively, because the gravitational lens effect integrates all the mass along the line of sight, and so unavoidably considers all the subclumps discussed here. For a more detailed discussion of the reason of the discrepancy between X-ray and lensing mass one has to wait for better X-ray data, e.g. a temperature determination from ASCA data, as well as deeper optical data, with the possibility to trace the cluster potential via weak lensing.

The total mass of $(1.5 \pm 0.8) \times 10^{14} M_\odot$ within 1 Mpc which is about the virial radius according to the spherical collapse approximation (Gunn & Gott 1972; White et al. 1993a) is a relatively low value compared to the typical mass range of clusters of $5 - 50 \times 10^{14} M_\odot$ (Böhringer 1995). It is an order of magnitude lower than the mass of the nearby clusters Coma and Perseus (Böhringer 1994). The gas mass fraction of 30^{+30}_{-10}% inferred from this number is at the upper limit of the typical range for clusters of 10-30% (Böhringer 1995). This high fraction makes Cl 0050-24 another example for the so-called baryonic catastrophe (Briel et al. 1992; White et al. 1993b).

Combined, all the arguments mentioned above point into the direction that Cl 0500-24 consists of two concentrations with little direct interaction. Only one of the subclusters has X-ray emission. But even considering the fact that only part of the optically visible cluster is associated with the X-ray properties, the values for the X-luminosity and the derived total mass are comparably small.

Acknowledgements. It is a pleasure to thank Hans Böhringer, Makoto Hattori, Andreas Huss, and Doris Neumann for helpful discussions. We also thank Leopoldo Infante for providing unpublished galaxy data to us, and Edmond Giraud for providing us with the unpublished redshift of the arc in Cl 0500-24. We acknowledge valuable comments by Jean-Paul Kneib which helped to improve the paper considerably. S.S. acknowledges financial support by the Verbundforschung.

References

Abell G., Corwin Jr. H.G., Olowin R.P., 1989, ApJS 70, 1
Arnaud M., Rothenflug R., Boulade O., Vigroux L., Vangioni-Flam E., 1992, A&A 254, 49
Bautz M.W., Mushotzky R., Fabian A.C., Yamashita K., Gendreau K.C., Arnaud K.A., Crew G.B., Tawara Y., 1994, PASJ 46, L131
Böhringer H., 1994, in: X-Ray Clusters of Galaxies, NATO Advanced Science Institute Vol. 441, Seitter, W.C. (ed.) Kluwer, Dordrecht, p. 123
Böhringer H., 1995, in: Proceedings of the 17^{th} Texas Symposium on Relativistic Astrophysics and Cosmology, Böhringer H., Morfill G.E., Trümper J.E. (eds.), New York Academy of Sciences, New York, p. 67
Briel U.G., Henry J.P., Böhringer H., 1992, A&A 259, L31
Cavaliere A., Fusco-Femiano R., 1976, A&A 49, 137
David L.P., Slyz A., Jones C., Forman W., Vrtilek S.D., Arnaud K.A., 1993, ApJ 412, 479

Dickey J.M., Lockman F.J., 1990, ARA&A 28, 215
Dressler A., Oemler A., Butcher H.R., Gunn J.E., 1994, ApJ 430, 107
Edge A.C., Stewart G.C., 1991a, MNRAS 252, 414
Edge A.C., Stewart G.C., 1991b, MNRAS 252, 428
Fabricant D.G, McClintock J.E., Bautz M.W., 1991, ApJ 381, 33
Giraud E., 1988, ApJ 334, L69
Giraud E., 1990, A&AS 83, 1
Giraud E., 1996, private communication
Griffith M.R., Wright A.E., Burke B.F., Ekers R.D., 1994, ApJS 90, 179
Gunn J.E., Gott J.R., 1972, ApJ 176, 1
Huss A., Jain B., Steinmetz M., 1996, in preparation
Infante L., Fouqué P., Hertling G., Way M.J., Giraud E., Quintana H., 1994, A&A 289, 381
Jones C., Forman W., 1984, AJ 276, 38
Koo D.C., 1981, ApJ 251, L75
Lea S.M., Henry J.P., 1988, ApJ 332, 81
Mellier Y., Soucail G., Fort B., Mathez G., 1988, A&A 199, 13
Neumann D.M., Böhringer H., 1996, MNRAS, submitted
Ohashi T., 1995, in: Seventeenth Texas Symposium on Relativistic Astrophysics and Cosmology, Böhringer H., Morfill G.E., Trümper J.E. (eds.), New York Academy of Sciences, New York, p. 217
Schindler S., Böhringer H., 1993, A&A 269, 83
Schindler S., Müller E., 1993, A&A 272, 137
Schindler S., Wambsganss J., 1996, A&A 313, 113
Trümper J., 1983, Adv. Space Res. 2, 142
Wambsganss J., Giraud E., Schneider P., Weiss A., 1989, ApJ 337, L73
White D.A., 1996, in: Röntgenstrahlung from the Universe, Zimmermann H.U., Trümper J.E., Yorke H., MPE report 263, p. 621
White S.D.M., Efstathiou G., Frenk C.S., 1993a, MNRAS 262, 1023
White S.D.M., Navarro J.F., Evrard A.E., Frenk C.S., 1993b, Nat 366, 429

This article was processed by the author using Springer-Verlag LaTeX A&A style file *L-AA* version 3.